

Article

# Macadamia Nutshell Biochar for Nitrate Removal: Effect of Biochar Preparation and Process Parameters

Salam Bakly<sup>1</sup>, Raed A. Al-Juboori<sup>1,2,\*</sup>  and Les Bowtell<sup>1</sup> 

<sup>1</sup> School of Civil Engineering and Surveying, Faculty of Health, Engineering and Sciences, University of Southern Queensland, West Street, Toowoomba, Queensland 4350, Australia

<sup>2</sup> School of Science, Engineering and Information Technology, Federation University Australia, University Drive, Mt Helen, VIC 3350, Australia

\* Correspondence: RaedAhmed.Mahmood@usq.edu.au; Tel.: +61-413-424-126

Received: 29 June 2019; Accepted: 5 August 2019; Published: 8 August 2019



**Abstract:** Agricultural runoff is a major cause of degradation to freshwater sources. Nitrate is of particular interest, due to the abundant use of nitrogen-based fertilizers in agricultural practices globally. This study investigated the nitrate removal of biochar produced from an agricultural waste product, macadamia nutshell (MBC). Kinetic experiments and structural analyses showed that MBC pyrolysed at 900 °C exhibited inferior NO<sub>3</sub><sup>-</sup> removal compared to that pyrolysed at 1000 °C, which was subsequently used in the column experiments. Concentrations of 5, 10 and 15 mg/L, with flowrates of 2, 5 and 10 mL/min, were examined over a 360 min treatment time. Detailed statistical analyses were applied using 2<sup>3</sup> factorial design. Nitrate removal was significantly affected by flowrate, concentration and their interactions. The highest nitrate removal capacity of 0.11 mg/g MBC was achieved at a NO<sub>3</sub><sup>-</sup> concentration of 15 mg/L and flowrate of 2 mL/min. The more crystalline structure and rough texture of MBC prepared at 1000 °C resulted in higher NO<sub>3</sub><sup>-</sup> removal compared to MBC prepared at 900 °C. The operating parameters with the highest NO<sub>3</sub><sup>-</sup> removal were used to study the removal capacity of the column. Breakthrough and exhaustion times of the column were 25 and 330 min respectively. Approximately 92% of the column bed was saturated after exhaustion.

**Keywords:** macadamia nutshell biochar; nitrate; statistical analyses; column experiments; kinetic experiments; adsorption capacity

## 1. Introduction

Contamination of freshwater sources is a serious issue worldwide. One of the main contributors to the contamination is agricultural runoff. It is of particular concern given the high level of nutrients contained, such as phosphorus and nitrogen compounds [1,2]. Nitrogen compounds such as nitrate can be problematic due to the widespread use of nitrogen based fertilizers and soil instability [3]. Nitrogen fertilizers undergo several chemical transformation processes such as ammonification, nitrification, de-nitrification, nitrogen fixation and immobilization in soil [4]. Nitrate is produced during nitrification, which is regarded as one of the fastest reaction pathways. Nitrate has a weak affinity to form surface complexes and this makes it readily available for dissolution into agricultural runoff [5].

The release of nitrate into freshwater bodies can cause detrimental quality problems for water. A high concentration of nitrate causes eutrophication, which can damage the ecosystem of the water bodies [6]. Nitrate can also pose a threat to human health as it has been linked to cancer and methemoglobinemia in infants [7]. In addition, nitrate leaching from agricultural fields can cause a significant impost for farmers, especially as only 30–50% of nitrogen compounds are normally taken up by crops [8] and the rest wasted in runoff events. Thus, it is important to develop cost effective

and environmentally friendly treatment techniques for agricultural runoff, not only to remove nitrates, but also to recover these nutrients where possible for reuse in agriculture.

Several treatment methods have been proposed for removing nitrate from aqueous solutions such as anion exchange, biological, chemical and catalytic denitrification, reverse osmosis and electrodialysis [4]. However, these methods were found to be cost ineffective, not suitable for large-scale applications and to generate hazardous by-products [9]. Adsorption techniques can address the aforementioned shortcomings [10] and possibly meet the criteria of nitrate recovery. What makes this technique most attractive is the possibility of using agricultural waste for preparing adsorbents [3].

The macadamia nut industry has been used as a case study in this investigation. Australia is the world's largest producer of macadamia nuts. The yearly production of this nut is approximately 50,000 tonnes in-shell, which is equivalent to 15,000 tonnes in kernel form [11]. This means that 35,000 tonnes of nut shell are produced yearly in Australia alone. The annual world production of Macadamia kernel is estimated to be 44,000 tonnes [12]. If the same proportion of nutshell reported in Australia is applied to this figure, more than 120,000 tonnes of macadamia nutshell is produced globally. This is a considerable amount of solid waste that needs to be put into a useful application to serve the agriculture sector [13]. This study proposes the use of macadamia nutshell biochar as an adsorbent for nitrate removal from agricultural runoff.

Macadamia nutshell biochar has been applied in several applications such as steel production [14], nutrient mobility control and soil amendment in agriculture [15,16] and denitrification in bioreactors in combination with other plant-waste biochars [17]. However, studies on the use of macadamia nutshell biochar solely for nitrate removal in kinetics and column experiments seem to be scarce. In most cases, macadamia nutshell (MBC) was used for nitrate removal in bioreactors [18] or was amended by coating with different chemicals [19]. While investigating such aspects is an important contribution to the field of knowledge, it is important to explore the capacity of unmodified MBC for nitrate removal in kinetics and column experiments, as this would inform future studies for further removal improvements. This study aims to fill this gap by thoroughly investigating the use of macadamia nutshell biochar produced at 900 °C and 1000 °C for nitrate removal from synthetic samples at a concentration range similar to that commonly present in agricultural runoff. Kinetic experiments and structural analyses were utilised to identify the best quality biochar. Statistical analyses were applied to study nitrate removal behavior under different treatment scenarios using column setup. Column removal capacity and other characteristics were determined based on the breakthrough curve of the column.

## 2. Materials and Methods

### 2.1. Solution Preparation

A synthetic solution was prepared by dissolving 135.4 mg sodium nitrate (M.W. = 84.99, analytical reagent) in 1 L of distilled water to produce a 100 mg/L nitrate concentration (stock solution). Three concentrations of 5, 10 and 15 mg/L  $\text{NO}_3^-$  were applied in this study. The concentration range was chosen to cover the minimum and maximum nitrate levels expected in agricultural runoff. In most parts of the world, for example China and the USA, the maximum nitrate concentration in many sites reaches up to 15 mg/L, while the lower limit is found to be in the range of 3–5 mg/L [20,21]. A study of 360 storm water sites around the USA targeting nitrate concentration found that the median limit was around 14 mg/L [22]. In addition, a report of the Department of Primary Industries indicated that the suitable  $\text{NO}_3^-$  for most plants is less than 10 mg/L [23]. This data informed the selection of concentration levels: a minimum level of 5 mg/L and maximum level of 15 mg/L, and their midpoint of 10 mg/L.

### 2.2. MBC Preparation

The feedstock was prepared from macadamia nutshell as a biochar module due to its availability, affordability, being a recycled product of agricultural waste and having a high surface area compared

to other nut shells such as pistachio, pecan, hazelnut and almond [24]. Macadamia nutshell was placed in a stainless-steel square container with a lid on ( $17.78 \text{ W} \times 16.51 \text{ L} \times 10.16 \text{ H cm}^3$ ) and pyrolysed using a kiln (Rio Grande PMC Model #703-118, Rio Grande, Albuquerque, NM, USA). The kiln was programmed for slow pyrolysis process conditions to drive the internal chamber to two temperatures  $900 \text{ }^\circ\text{C}$  and  $1000 \text{ }^\circ\text{C}$  at a rate  $600 \text{ }^\circ\text{C/h}$  and holding time for an hour before cooling down to room temperature. Macadamia nutshell normally loses about 65% of mass in the range  $260\text{--}400 \text{ }^\circ\text{C}$  due to conversion to biochar [14]. Using higher temperatures to pyrolyse the biomass has the advantage of reducing volatiles, obtaining more stable carbon with a high surface area [25]. After pyrolysis completion, MBC was cooled and later was gently crushed using a hand grinder (Weston). The crushed MBC was then sieved through a  $1.18\text{--}2.30 \text{ mm}$  sieve as this size range was found to be effective for sorption [26]. After that, the MBC obtained from the above steps was rinsed with distilled water for two hours to remove any impurities such as ash. Following this step, the MBC was autoclaved at  $121 \text{ }^\circ\text{C}$  and pressure of 2.50 bars for steam activation using a Hirayama Manufacturing Corporation autoclave (Model HV-50L, Hirayama, Toyono, Japan). Steam activation was applied to achieve wide pores in the prepared MBC [27]. Given that biochar is a suitable environment for microbial growth, applying steam to freshly produced biochar can also ensure the inhibition of such activities which may affect nitrate removal. The final product was then dried and stored in plastic containers to be used in adsorption experiments.

### 2.3. Column Preparation

The components of the column are illustrated in Figure 1. A plastic column that carries a bed height of  $12.20 \text{ cm}$  and an internal diameter of  $3.85 \text{ cm}$  was used for carrying out column experiments. The column was rinsed with deionized water (DIW), sterilised with ethanol ( $\text{C}_2\text{H}_5\text{OH}$ ). A circular fiberglass mesh was laid at the bottom of the column. The column was packed with  $60 \text{ g}$  of MBC prepared at the chosen pyrolysis temperature based on preliminary experiments, which will be explained later in Section 3. Once the column was packed with the MBC, the top of biochar was covered with filter paper of  $0.45 \text{ }\mu\text{m}$  size to ensure uniform distribution of water in the column. The two ends of the column were covered with plastic caps and sealed with commercial silicon. The two caps have openings to accommodate the hosing of the feed and discharge lines.

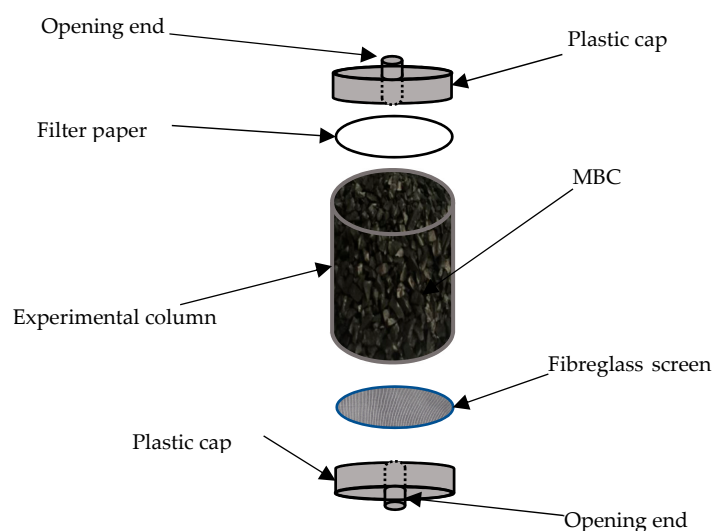


**Figure 1.** Schematic diagram of macadamia nutshell (MBC) column design.

## 2.4. Analytical Measurements

### 2.4.1. Morphology and Elemental Composition

A JOEL scanning electron microscope (SEM) (JCM-6000 Benchtop SEM, JOEL Ltd, Tokyo, Japan) was used for visual comparison between the raw and pyrolysed macadamia nutshell. SEM images were taken at  $\times 1000$  magnification power. SEM is equipped with a secondary electron image (SEI) in a chamber with high vacuum pressure mode around  $10^{-2}$  pa in ten minutes and accelerating voltage of 5 kV.

### 2.4.2. Functional Groups

A Shimadzu 206-97505D/2015 Fourier transform infrared spectrophotometer (FTIR, Shimadzu, Kyoto, Japan) was used to examine the MBC structure at different conditions (pyrolysis temperatures and before and after adsorption). FTIR measurements were utilised to monitor the change in functional groups available on the char surface as it is considered to be a sensitive tool for detecting any change that might occur in the composition of the functional groups on the surface of the biomass [28]. The average record spectra was chosen from the upper limit bands at  $4000\text{ cm}^{-1}$  to the lower bands at  $400\text{ cm}^{-1}$  [29]. Each band number could be assigned to a specific chemical bond and could help in understanding the MBC removal mechanisms of nitrate. The applied FTIR measurement conditions were as follows: % transmittance mode, no. of scans = 45, Happ-Genzel apodization and resolution of  $4\text{ cm}^{-1}$ .

A 2 mg MBC sample was ground using a mortar and pestle and mixed with 200 mg potassium bromide (KBr) to 0.1 wt.%. The mixture was pressed into a pellet of 15 mm diameter and 1 mm thickness using a manual hydraulic press approximately 8–9 kPa for 0.5 min [19]. The pellet was then placed in the FTIR instrument for a scanning test.

### 2.4.3. X-ray Diffraction Measurements

XRD analyses were obtained on a Panalytical X'Pert Pro diffractometer (Malvern Panalytical, Malvern, UK) at Federation University Australia equipped with an incident beam BBHD Co K $\alpha$  monochromator and an X'Celerator linear detector, operated at 40 kV and 25 mA over  $5^{\circ}$ – $70^{\circ}$   $2\theta$  with a step size of  $0.017^{\circ}$   $2\theta$  at a rate of  $0.08^{\circ}$   $2\theta$  per second.

### 2.4.4. Elemental Composition

The weight and atomic percentage of the components of raw and pyrolysed macadamia nutshell at  $900^{\circ}\text{C}$  and  $1000^{\circ}\text{C}$  were determined using the Phenom ProX Desktop scanning electron microscope (ThermoFisher, Melbourne, Australia).

### 2.4.5. Nitrate Measurements

An Ion Chromatography System ICS-2000 instrument (Dionex-Thermo Fisher, Melbourne, Australia) was used to measure nitrate concentration in the samples before and after treatment. ICS-2000 works on comparing the samples to a three-point calibration curve applying the standard method 4110B [30]. Five millilitre plastic vials with filter cap ( $20\text{ }\mu\text{m}$ ) were used for carrying samples. The results obtained from the ICS-2000 in the form of  $\text{NO}_3^-$ -N were converted to  $\text{NO}_3^-$  by multiplying by a factor of 4.428.

## 2.5. Kinetic Experiments

In this study, kinetic and column experiments were used to check the adsorption capability of MBC. All experiments were conducted in triplicate and a blank sample was analysed as a reference for each test. The results of kinetic experiments help in narrowing down the scope of the experimental parameters to be studied.

For the kinetic experiments, 10 mL from the stock solution was added to 90 mL of distilled water, to obtain a concentration of 10 ppm. This 100 mL solution was placed in a 250 mL Pyrex beaker with 1 g of MBC prepared at 900 °C and another beaker of 1000 °C MBC at a pH of 5.5 (determined to be the best pH level for removal through preliminary testing) at a temperature of 20.9 °C to compare the two. The solution was stirred for 48 h to obtain the best equilibrium contact time between the solution and MBC particles, which estimates the maximum potential of the MBC for effective removal of nitrate. Samples were collected at various time intervals and filtered directly using a 0.45 µm paper filter to stop any reaction between the solution and MBC. The filtrate was then used for nitrate measurements.

## 2.6. Column Experiments

The column presented in Figure 1 was used for conducting column experiments. After packing the column with MBC, it was rinsed with Deionised Water (DIW) several times until the leachate pH settled at a certain level indicating that the column was clean and ready for use [31]. This also ensures that a minimal amount of elements would be released from the biochar during the experiments. In this process, upward and downward flow through the column was tested for preliminary experiments to choose the most effective flow direction.

All of the experiments discussed below were conducted in triplicate to improve the accuracy and repeatability of the experiments. Figure 2 demonstrates the experimental set-up of the column experiments. Twenty-litre, sterilised plastic containers were used to carry the feed solution with three different NO<sub>3</sub><sup>-</sup> concentrations of 5, 10 and 15 ppm. The feedwater was pumped in a single stage into the column through silicon tubing at three different flowrates of 2, 5 and 10 mL/min using a Masterflex peristaltic pump (model no. 7520-47, USA) and an ISMATEC ecoline pump (model ISM1076A, Germany). Samples were collected periodically to obtain the optimum removal time. Nitrate was measured using the ICS-2000 as explained in the previous section. Equations (1) and (2) were used to calculate the percentage removal (%) and removal capacity denoted as  $q_t$  (mg/g MBC), respectively.

$$\text{Nitrate removal (\%)} = \frac{\text{Nitrate conc.in feed water} - \text{Nitrate Conc.in column leachate}}{\text{Nitrate conc.in feed water}} \times 100, \quad (1)$$

$$q_t = \frac{\text{Nitrate conc.in feed water} - \text{Nitrate Conc.in column leachate}}{\text{Nitrate conc.in feed water}} \times \text{solution volume}, \quad (2)$$

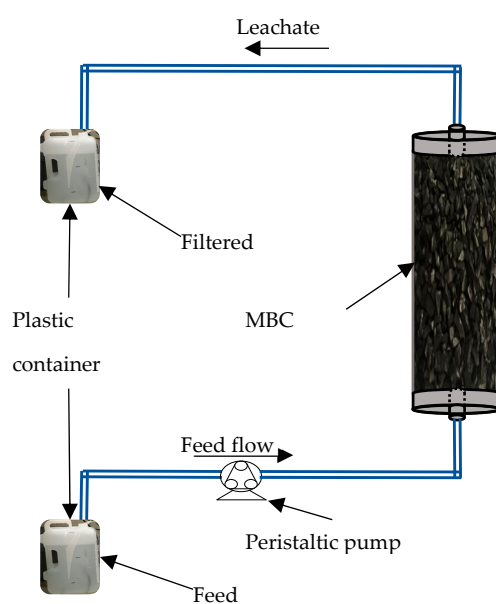


**Figure 2.** Column experiments process.

### 2.7. Statistical Analyses

Experimental design and data analyses were carried out using MINITAB 17 software. The order of the experiments was randomised to obtain a normal distribution of the experimental errors. Three nitrate concentration levels and three flowrate levels were used to construct a 2<sup>3</sup> factorial design. Each experiment was conducted in triplicate and samples were collected after six hours.

## 3. Results and Discussion

### 3.1. Kinetic Experiments—Effect of Pyrolysis Temperature

Figure 3 shows the average nitrate removal for MBC prepared under two different temperatures 900 °C and 1000 °C. It can be seen that MBC reaches saturation after 2 h at 0.095 and 0.057 mg/g MBC for 1000 °C and 900 °C, respectively. Nitrate removal after 24 h was checked and found to be in the same level as that of 2 h. These results agree with the finding reported in [32] where nitrate adsorption by biochar produced from agricultural waste was the highest in the first few hours and then plateaued out. One can easily notice from Figure 3 that MBC prepared at 1000 °C exhibited better NO<sub>3</sub><sup>-</sup> removal, as opposed to that prepared at 900 °C. The trend of nitrate removal with MBC prepared at 1000 °C was tested against pseudo-first and -second order adsorption kinetics, applying Equations (3) and (4), respectively [32,33]. It was found that the nitrate adsorption was better described with a pseudo-second order approximation, as demonstrated in Figure 4 and Table 1.

$$q_t = q_e(1 - e^{-k_1t}), \tag{3}$$

$$q_t = \frac{q_e^2k_2t}{1 + q_ek_2t}, \tag{4}$$

where  $q_e$  is nitrate removal capacity at equilibrium (mg/g MBC),  $k_1$  and  $k_2$  are the first- and second-order sorption rate constants (min<sup>-1</sup>) and  $t$  is time (min).

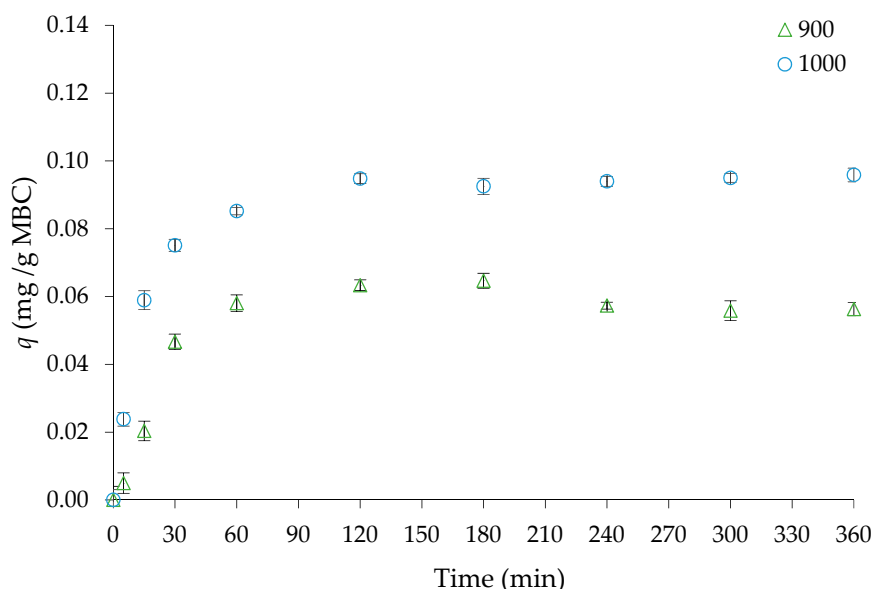
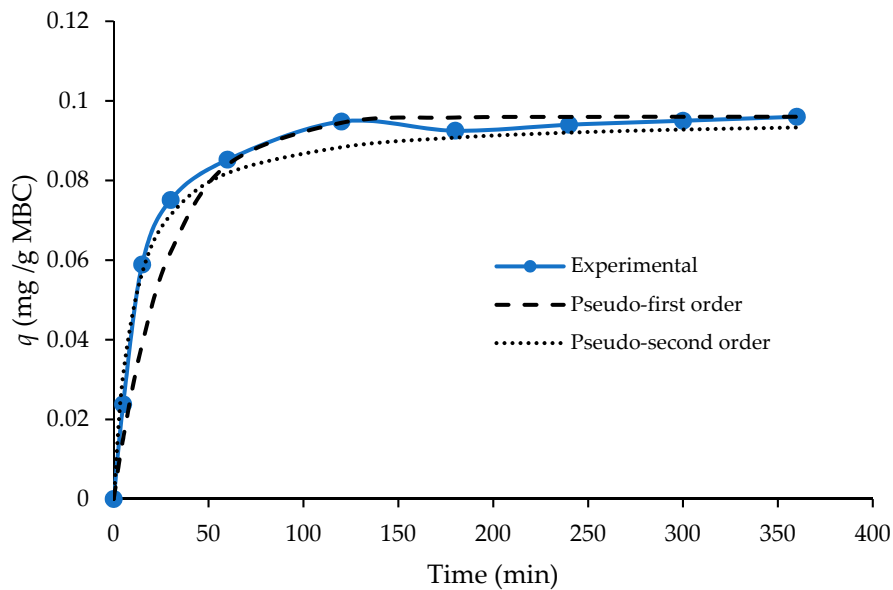


Figure 3. Nitrate removal with kinetic experiments for MBC prepared at 900 °C and 1000 °C.

Table 1. Adsorption kinetic models for nitrate removal with MBC prepared at 1000 °C.

Pseudo-First Order Model			Pseudo-Second Order Model		
$q_e$ (mg/g MBC)	$K_1$ (min <sup>-1</sup> )	$R^2$	$q_e$ (mg/g MBC)	$K_2$ (min <sup>-1</sup> )	$R^2$
0.96	0.0328	0.92	0.93	1.004	0.98



**Figure 4.** Nitrate adsorption: pseudo-first and -second kinetics vs. experimental.

The high nitrate removal with MBC prepared at 1000 °C compared to 900 °C instigated the investigation of the structural differences between the two samples. Hence, morphological, chemical structure and crystallinity measurements were conducted. Figure 5 shows the SEM images of raw (A) and pyrolysed macadamia nutshell at 900 °C (B) and 1000 °C (C). It can be noticed that the raw macadamia nut shell surface structure has packed pores with organic materials in contour pattern. Pyrolysing the nutshells opened up the pores, however the density, size and uniformity of pores of MBC at 1000 °C are better compared to that produced at 900 °C.

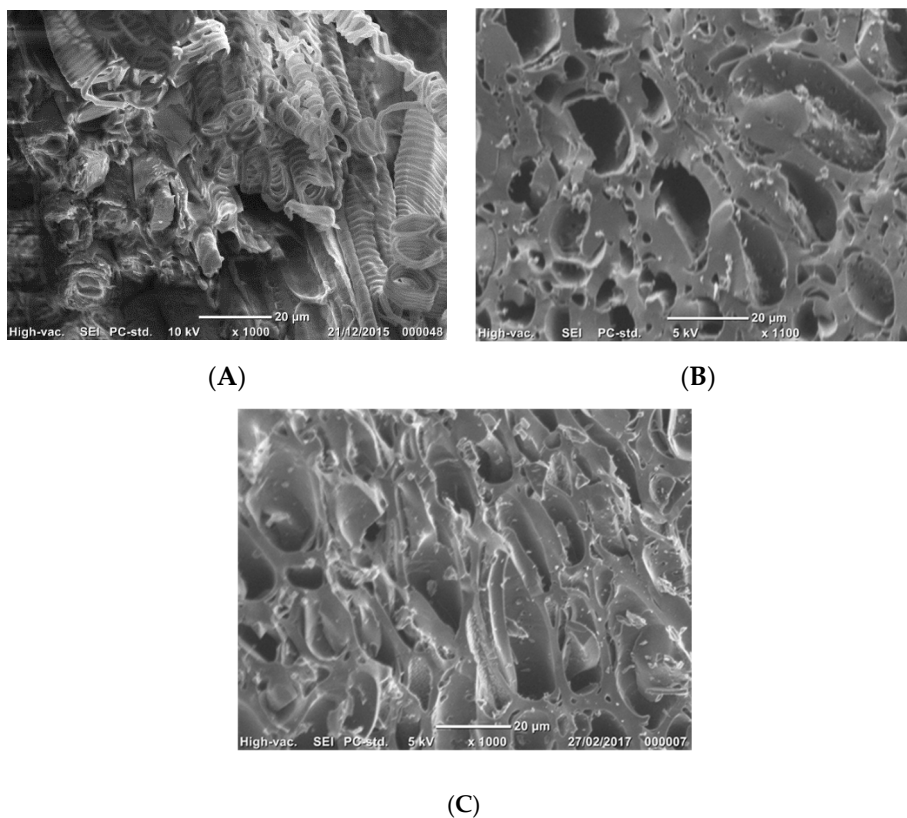


**Figure 5.** SEM for raw macadamia nut shell (A) and pyrolyzed at 900 °C (B) and 1000 °C (C).

Figure 6 shows the weight and atomic percentage of the components of raw and pyrolysed macadamia nutshell at 900 °C and 1000 °C, using the Phenom ProX Desktop scanning electron microscope. There is a difference in terms of the weight and atomic percentages of the main elements of carbon and oxygen for the raw macadamia nutshell and MBC. It is worth mentioning that raw macadamia nutshell contains small amounts of inorganics such as Na and Ca, which are not shown in Figure 6B,C as they are almost completely diminished when pyrolyzed at 900 °C or 1000 °C. It is clear that the carbon percentages increased while other elements decreased in both weight and atomic percentages as the temperature rose. In the pyrolysis process, the carbon percentage was increased, driving off all the volatile materials including the oxygen contained in the raw shells. The carbonisation process can cause the volatilisation of noncarbonated elements and development of pore structures as shown in Figure 5. A similar process of change in the char morphological structure and volatile compounds was reported in other studies that used macadamia nut shell waste and pyrolysis at 700 °C [34]. The loss of oxygen with temperature increase may be attributed to loss in oxygen containing functional groups and this can be confirmed using the FTIR technique.

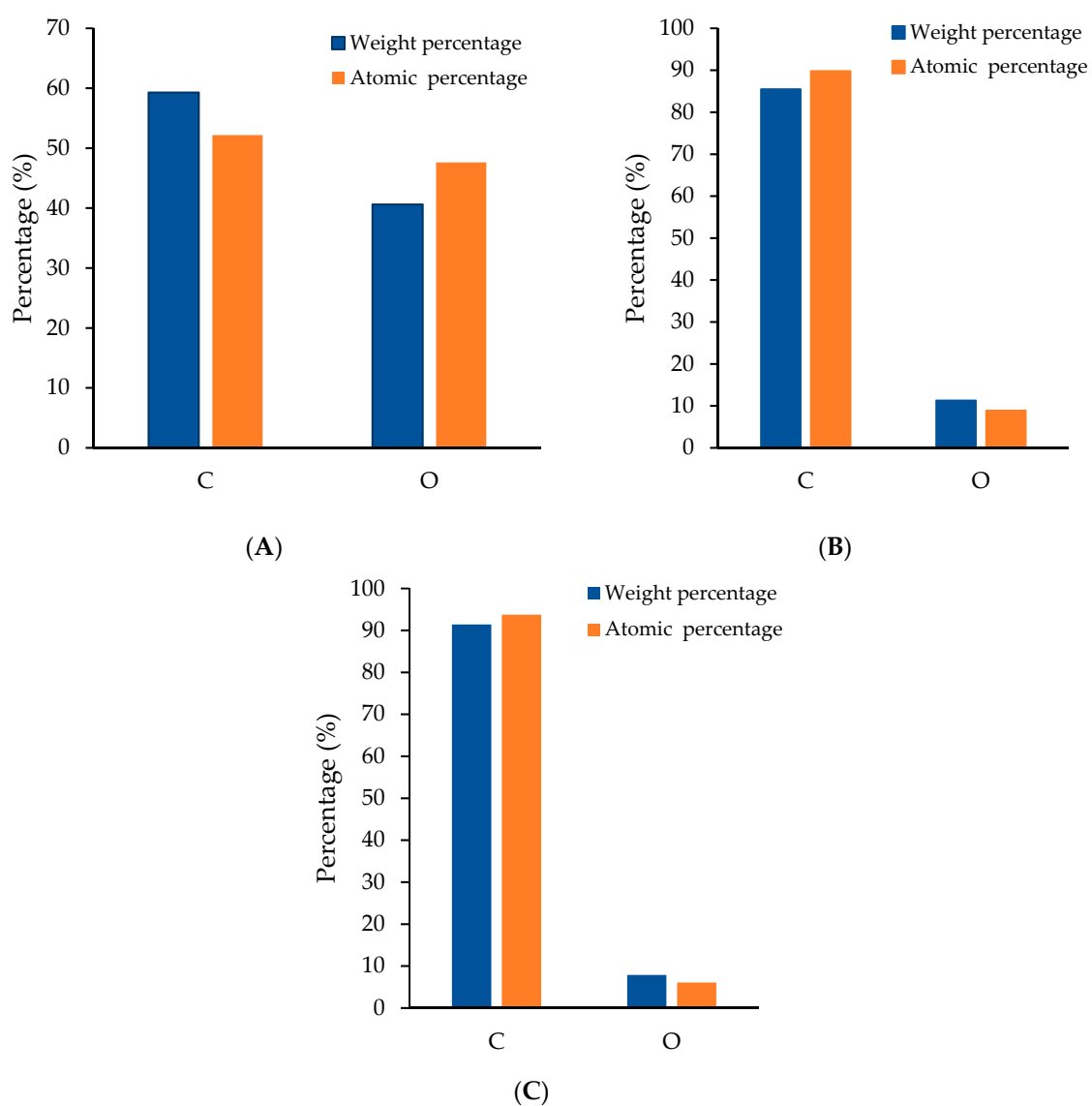


**Figure 6.** Weight and atomic elements percentage of raw macadamia nut shell (A) and MBC prepared at 900 °C (B) and 1000 °C (C); Na and Ca are detected in small amounts (0.2 and 0.001) in raw material but not at all at 900 °C and 1000 °C.

FTIR spectra of MBC prepared at the two studied temperatures are depicted in Figure 7. Both have the same peak positions, which means they have similar functional groups that allow them to adsorb similar elements [35]. The intensity of the peaks for 1000 °C are less than those for 900 °C. The peak at 3454 cm<sup>-1</sup> indicates the presence of an -OH in a carboxylic group [36]. Peaks between 1000 and 1100 cm<sup>-1</sup> are associated with C-O and -OH groups [37]. The decrease in the intensity correlates well with the compositional analyses of biochar in Figure 7, as both results indicate loss of oxygen containing functional groups with increasing pyrolysis temperatures. Given that one of the nitrate removal mechanisms with biochar is interaction with functional groups, higher nitrate removal with MBC prepared at 1000 °C can be explained by the increase in surface roughness (Figure 5) and conductivity as nitrate removal by biochar is influenced considerably by electrostatic interactions [38]. FTIR analyses of MBC prepared at 1000 °C before and after nitrate adsorption were performed and the spectra are depicted in Figure 8A. The intensity of all identified prominent peaks decreased substantially after nitrate adsorption, reflecting MBC structural alterations caused through functional group and electrostatic interactions.

Figure 8B shows the second derivative FTIR spectrum of MBC prepared at 1000 °C before and after nitrate adsorption. The second derivative was applied to track the functional groups that are mostly affected by nitrate removal. Previous studies reported that the hydroxyl group is the main functional group that interacts with nitrate [32]. Figure 8B illustrates that the phenolic structure on the char represented by the peak at 1207 cm<sup>-1</sup> disappeared after nitrate adsorption. Despite the fact that the pure NO<sub>3</sub><sup>-</sup> did not react with phenol [39], the disappearance of the phenol peak may indicate conversion of NO<sub>3</sub><sup>-</sup> to NO<sub>2</sub> under a reduction process, followed by a reaction with phenol to produce nitrophenols. After combining the results from the pseudo-second-order model in Table 1 and the second derivative FTIR from Figure 8B, the likely mechanisms involved in the adsorption process are electron transfer between the adsorbent and the adsorbate and the physical interaction due to rough texture of the biochar as shown in Figure 5 [32,40].

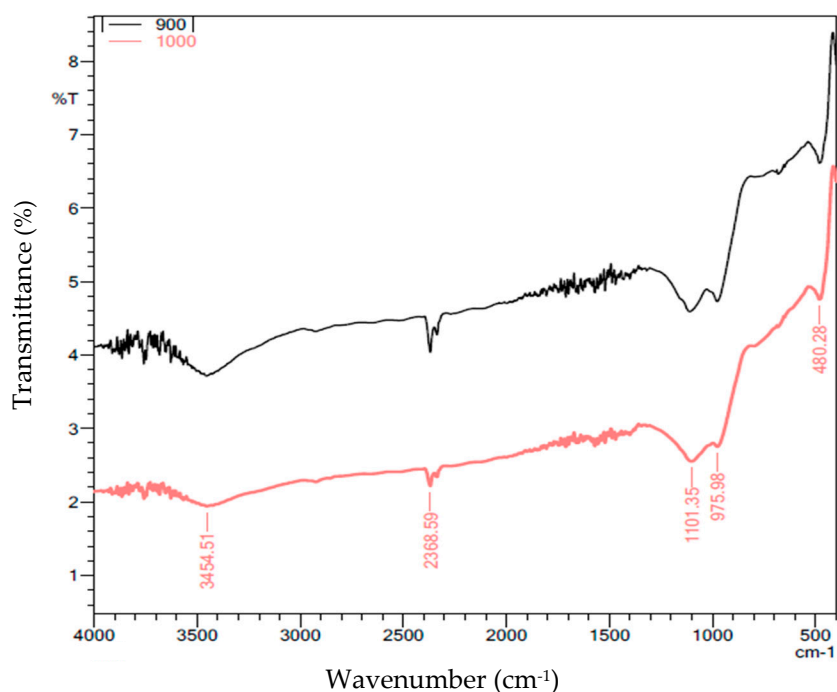
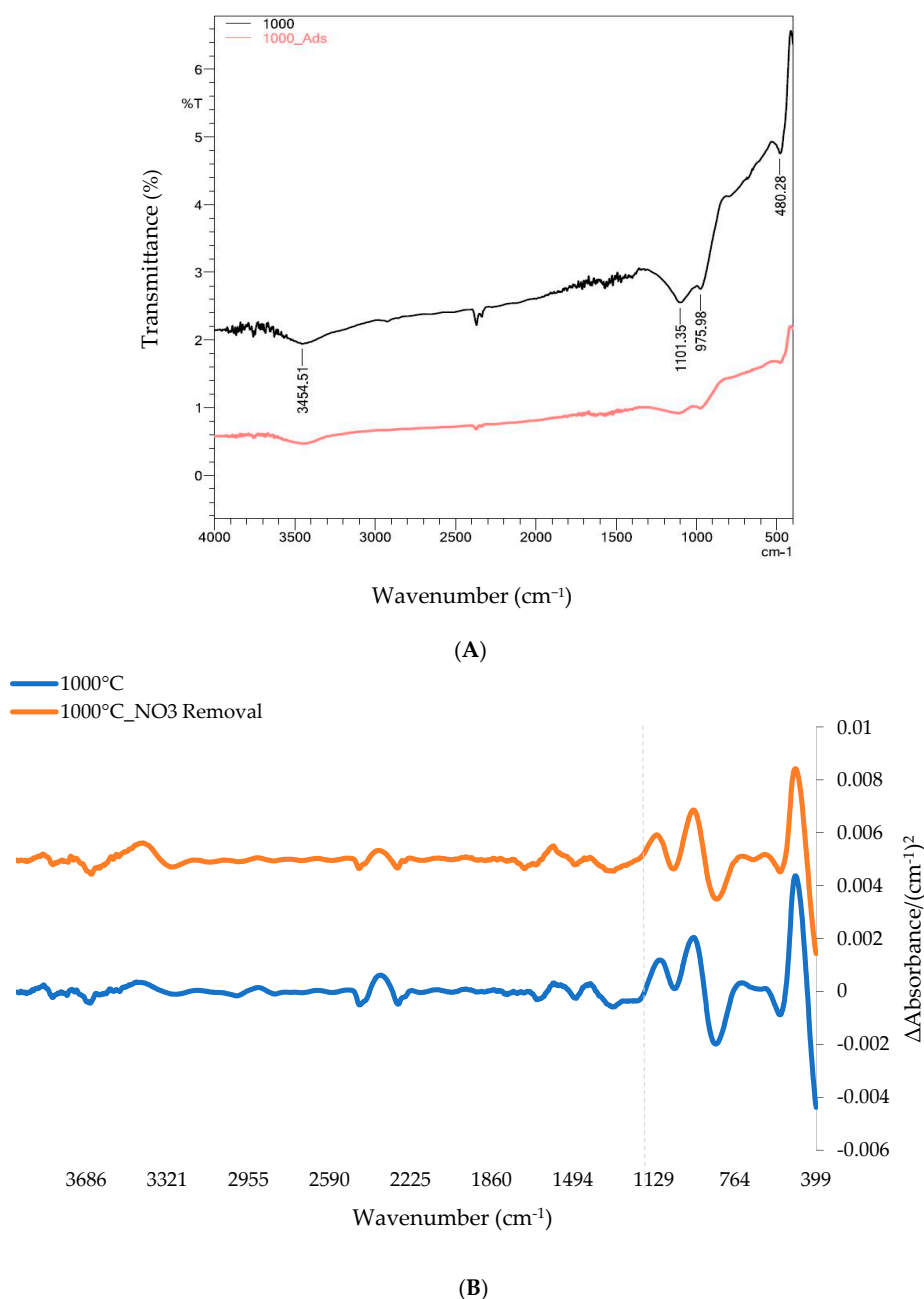


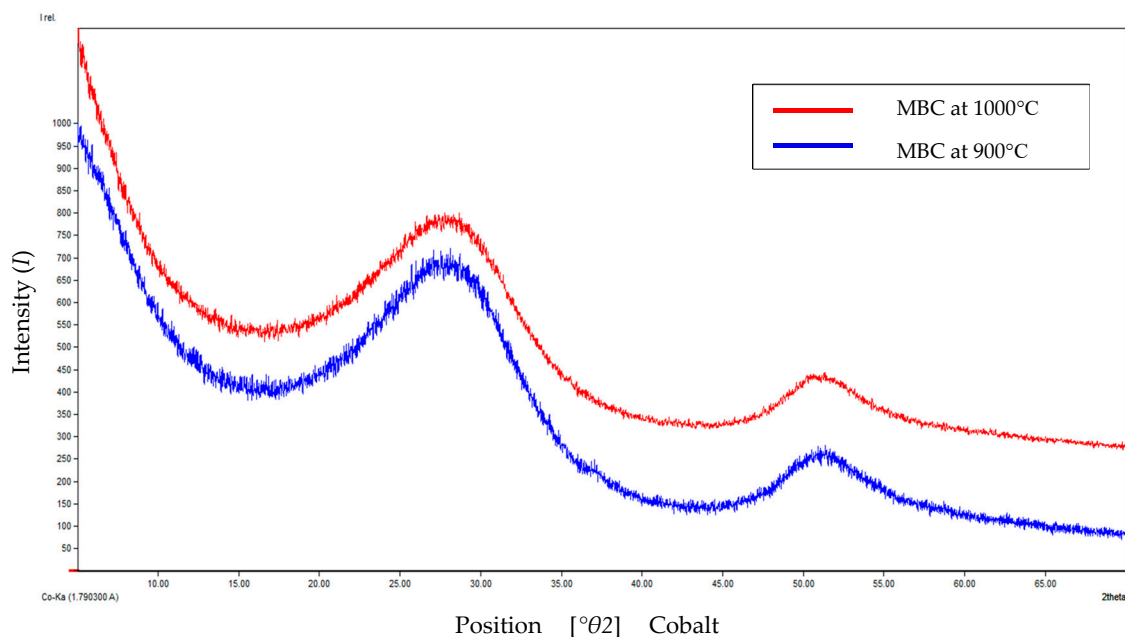
Figure 7. FTIR spectra for 900 °C and 1000 °C MBC.

The effect of pyrolysis temperature on biochar crystallinity was examined in this study using XRD analysis. Figure 9A shows the diffractograms of MBC prepared at 900 °C and 1000 °C. It can be noticed that increasing the temperature reduces the sharpness of the crystallinity characteristic

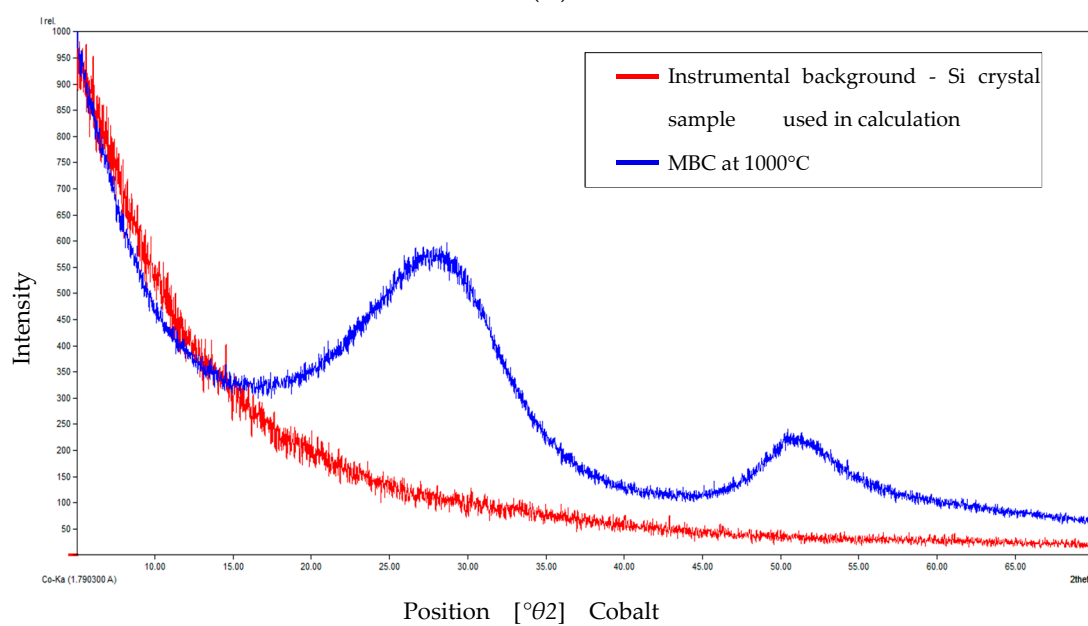
peak, which falls in  $\theta$  range of 25–30° and increases the intensity. Similar observations were reported in previous studies for biochar derived from agricultural waste (e.g., peanut shell) [41,42]. Degree of crystallinity and amorphous content of MBC were determined based on the peak area calculation of the char in relation to a high purity crystalline background following the method explained in [43] as demonstrated in Figure 9B. These calculations were conducted using the Scherrer calculator from Panalytical High Score Plus. Degree of crystallinity and amorphous contents of MBC at the two tested temperatures are presented in Table 2. It seems that crystallinity of MBC increases with increasing temperature and this is consistent with observations made by other studies [14,44]. It can be inferred from XRD analyses that nitrate removal increases with an increasing degree of crystallinity, and this agrees with the results obtained in [41].



**Figure 8.** FTIR spectra of MBC prepared at 1000 °C before and after nitrate adsorption (A) and the second derivative FTIR spectra of MBC prepared at 1000 °C before and after nitrate adsorption (B).



(A)



(B)

**Figure 9.** XRD spectra for MBC at 900 °C vs. 1000 °C (A) and MBC at 1000 °C vs. background (B).

**Table 2.** Degree of crystallinity and amorphous content of MBC.

Temperature	Degree of Crystallinity (%)	Amorphous Content (%)
900 °C	18.07	81.93
1000 °C	20.72	79.28

### 3.2. Column Experiments

#### 3.2.1. Preliminary Testing for Effect of Flow Direction on Nitrate Adsorption

The effect of flow direction in the column experiments was explored and the results are presented in Figure 10. It is clear that upward flow resulted in higher nitrate removal as opposed to the downward

flow approach. The upward-flow system removal rate started at around 80% for the first five minutes, while the downward system started at around 12% for the same period. Reaching the saturation point was slower with upward flow than with downward flow. Saturation of the upward flow started at around the fourth hour at 20%, while the downward system saturated earlier (in the first half an hour) at around 5%. These results show that upward flow is more efficient than the comparable downward flow. This could largely be due to the better solution distribution with the former compared to the latter. Preliminary results obtained so far show that MBC prepared at 1000 °C using upward flow results in higher nitrate removal, when compared to other tested parameters, and hence they were applied in the column experiments that followed.

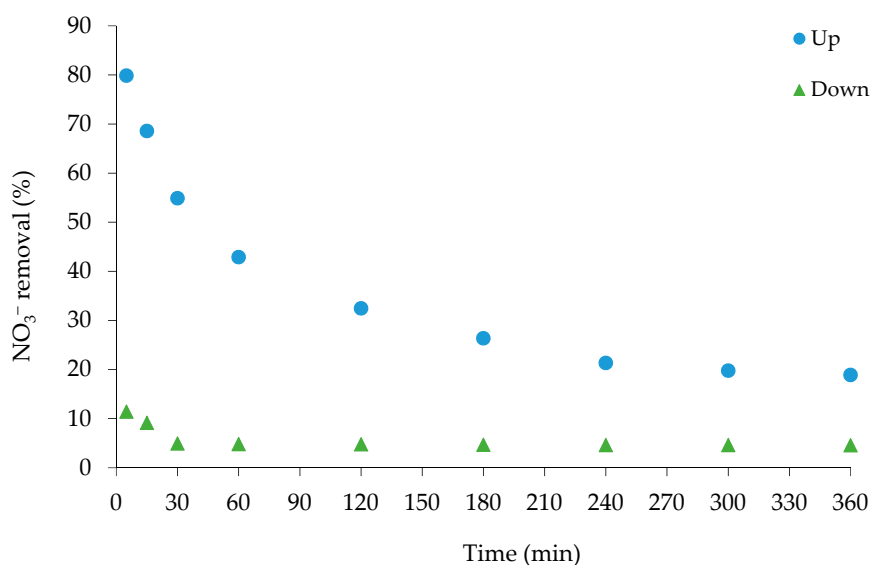


**Figure 10.** Upward and downward flow column adsorption experiment for 6 h.

### 3.2.2. Normality and Residual Analyses

Table 3 shows nitrate removal percentage and capacity with different treatment scenarios for 3 levels of tested flowrates and concentrations. In order to ensure a reasonable error distribution, experiments were conducted in a random manner. Each experiment was repeated three times.

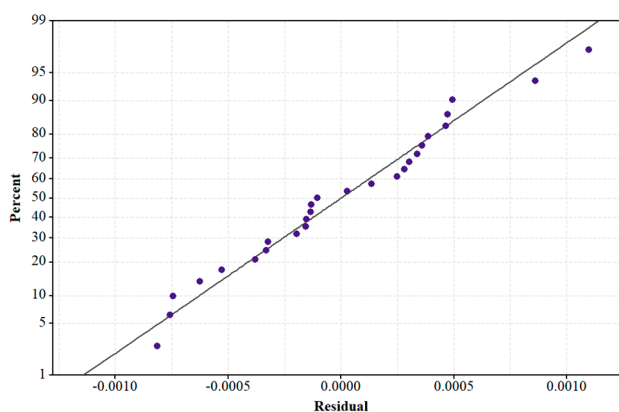
**Table 3.** Nitrate removal with different treatment scenarios.

No.	Flowrate (mL/min)	Nitrate Conc. (mg/L)	Nitrate Removal (%)	Removal NO <sub>3</sub> <sup>-</sup> mg/g MBC
1	10	5	42.73	0.04
2	2	5	43.36	0.04
3	10	10	28.59	0.05
4	2	10	46.84	0.07
5	2	10	59.40	0.09
6	2	15	38.82	0.10
7	4	10	31.26	0.07
8	4	10	35.77	0.06
9	2	15	45.83	0.11
10	2	5	38.95	0.07
11	2	10	46.13	0.07
12	4	15	21.77	0.05
13	4	10	32.16	0.05
14	10	10	26.71	0.04
15	4	5	42.30	0.03
16	10	5	29.81	0.03
17	4	15	29.48	0.07

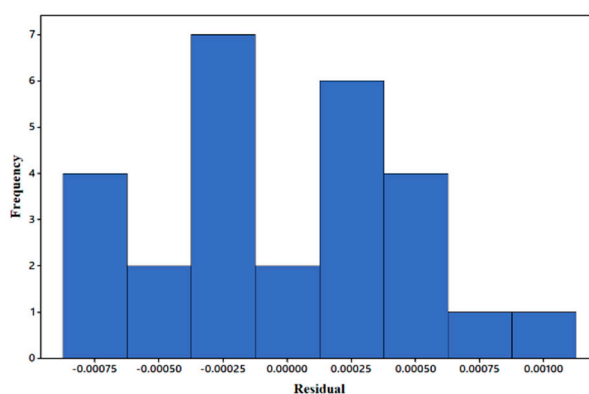
Table 3. Cont.

No.	Flowrate (mL/min)	Nitrate Conc. (mg/L)	Nitrate Removal (%)	Removal NO <sub>3</sub> <sup>-</sup> mg/g MBC
18	4	15	28.39	0.07
19	4	5	18.69	0.02
20	2	5	52.57	0.04
21	10	15	17.68	0.04
22	4	5	39.85	0.03
23	10	15	21.43	0.04
24	10	5	35.33	0.03
25	10	10	29.20	0.05
26	2	15	43.52	0.11
27	10	15	20.05	0.05

Prior to delving into the statistical analysis for the obtained nitrate removal levels, it is important to check that the errors are normally distributed and independent of external influence (e.g., experimenter errors). A number of statistical diagnostic tests were performed in this study and the results are presented in Figure 11. It can be seen that the errors are normally distributed, as shown by close distribution of residuals around the fitted regression line (Figure 11A) and bell-like shape histogram (Figure 11B) [45]. Figure 11 also shows that the data is independent of the order of the experiments and the errors are randomly distributed, indicated by the arbitrary patterns around zero in C and D [46].

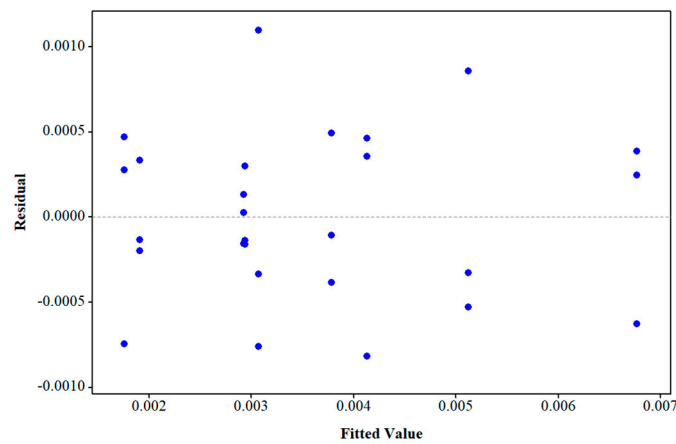


(A)

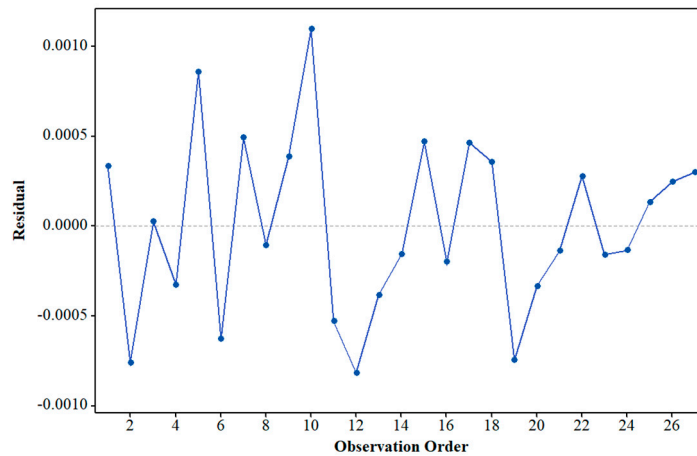


(B)

Figure 11. Cont.



(C)



(D)

**Figure 11.** Statistical diagnostic tests of nitrate removal: normal probability plot of residuals (A), residual vs. frequency (B), residuals vs. fitted values (C) and residuals vs. observation order (D).

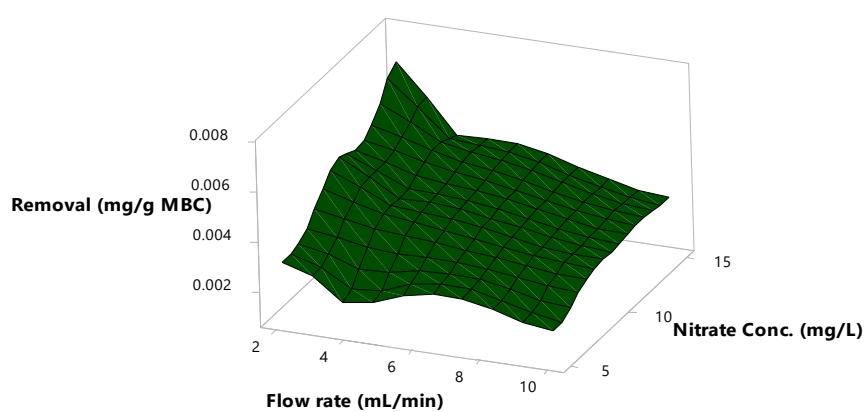
The significance of nitrate removal was tested at a confidence level of 0.95 ( $p$ -value = 0.05). The analysis of variance of nitrate removal is presented in Table 4. The model that best fit nitrate removal behaviour with the tested levels of flowrate and concentration is liner, indicated by a significant  $p$ -value. The main effects of flowrate and concentration had a significant effect on nitrate removal. The interactive effect of flowrate and concentration was also found to be significant, but to a lesser extent when compared to the main effects of the two factors.

**Table 4.** Analysis of variance (ANOVA) for  $\text{NO}_3^-$  removal.

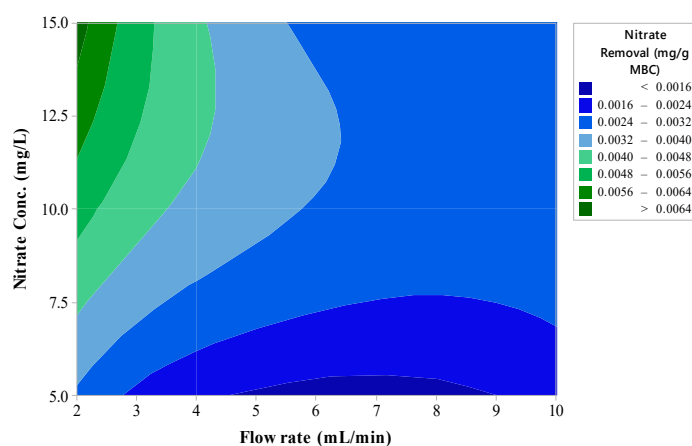
Source	DF	Adj SS	Adj MS	F-Value	$p$ -Value
Model	8	0.000060	0.000008	21.79	0.000
Linear	4	0.000055	0.000014	39.43	0.000
Flowrate (mL/min)	2	0.000028	0.000014	40.12	0.000
Nitrate Conc. (mg/L)	2	0.000027	0.000013	38.74	0.000
Flowrate (mL/min)*Nitrate Conc. (mg/L)	4	0.000006	0.000001	4.16	0.015
Error	18	0.000006	0.000000		
Total	26	0.000067			

### 3.2.3. Surface and Contour Plots Analyses

Surface and contour plots provide deeper insights into the behavior of the studied responses, for a combination of various levels of the studied factors [47]. The plots for nitrate removal response under three levels of flowrate and initial concentrations are shown in Figure 12. Nitrate removal increases with increasing initial concentration of nitrate in the solution, however the rate of increase is steeper at low flowrate compared to high flowrate. This is attributed to the fact that the contact time is higher with lower flowrate as opposed to high flowrate [48]. The increase in the initial concentration leads to a high nitrate deposition rate onto the packed char, and this in turn reduces the driving force of mass transfer, resulting in less adsorption [49]. The effect of flowrate on nitrate removal fluctuates at low concentration, while following a linear drop trend at high concentration, except for a palpable dip at 4 mL/min. This indicates that column configuration has inconsistent performance with low adsorbate concentration. Overall, the highest nitrate removal of 0.11 mg/L  $\text{NO}_3^-$  removed per gram of MBC was achieved with the lowest flowrate of 2 mL/min and highest concentration of 15 mg/L. These conditions will be applied in the next section to find the characteristics that define the capacity and effective operating time for column configuration.



(A)



(B)

**Figure 12.** Surface (A) and contour (B) plots for nitrate removal with MBC.

### 3.2.4. Effective Operation Conditions for Column

The results obtained in this study confirm that MBC is effective in removing nitrate. It is now important to find the effective design parameters for the MBC column configuration in order to allow replication on a large-scale setup. From a scalability perspective, the important design parameters for a biochar column are bed capacity (BC), breakthrough time ( $T_b$ ) and exhaustion time ( $T_s$ ). These can be

found by constructing the breakthrough curve of the column under the optimum removal conditions (2 mL/min and 15 mg/L) as shown in Figure 13. The area above the breakthrough curve represents the bed capacity and is given by Equation (5) [50].

$$BC = G \int_0^T (C_0 - C)dt, \tag{5}$$

Equation (5) can be integrated to a limit of  $T = T_s$  to produce the following equation:

$$BC = G (C_0 - C^*)T_s, \tag{6}$$

where  $G$  is the solution flowrate (L/min),  $C_0$  and  $C^*$  are nitrate inlet concentration and equilibrium concentration with fresh MBC (i.e., nitrate concentration in the column effluent at the first collection interval,  $\approx 1.6$  mg/L) and  $T_s$  is the time required for full bed exhaustion (min). The bed is considered exhausted when it reaches a stable very low removal percentage and the operation becomes energy inefficient. The exhaustion point in this study was selected to be  $C/C_0 = 0.8$ , where  $C$  is nitrate concentration at any time (mg/L).  $T_s$  is considered to be the corresponding time to this point as depicted in Figure 13 with a straight broken line. At this point, a significant portion of the column bed would be saturated and therefore would not contribute to nitrate adsorption. The portion is termed as equivalent length of unused bed (LUB), which is provided in Equation (7) [50].

$$LUB = \frac{Z}{T_s} (T_s - T_b), \tag{7}$$

where  $Z$  is the total bed height (cm) and  $T_b$  is the breakthrough time (min).  $T_b$  can be found from the breakthrough curve at  $C/C_0 = 0.2$ . The full bed characterisation of the MBC column is presented in Table 5.

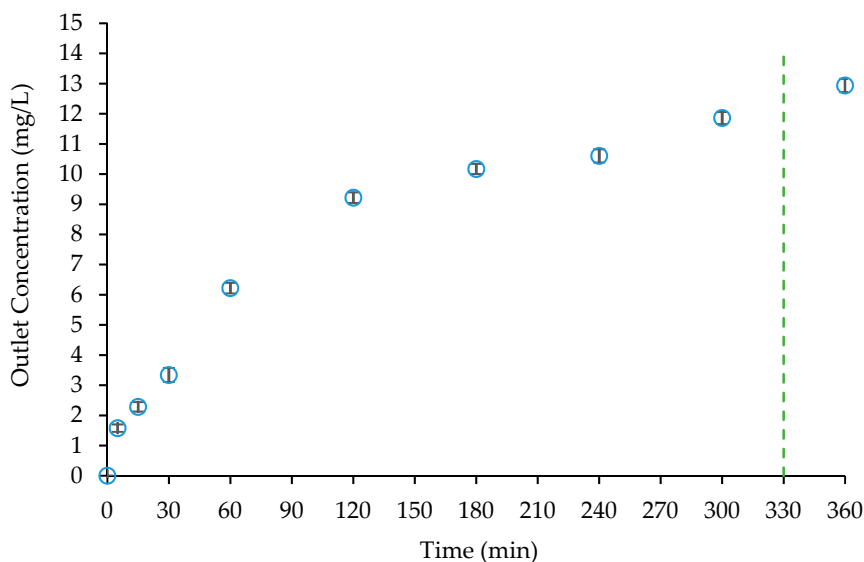


**Figure 13.** Breakthrough curve for nitrate removal in MBC column at feed flowrate of 2 mL/min and influent concentration of 15 mg/L.

**Table 5.** MBC bed characterisation for  $\text{NO}_3^-$  at feed flowrate of 2 mL/min and influent concentration of 15 mg/L.

Adsorbent Weight (g)	$T_s$ (min)	$T_b$ (min) at $C/C_0 = 0.20$	LUB (cm)	Amount Adsorbed at $T_b$		Amount Adsorbed at Full Bed Exhaustion	
				Total (mg)	mg/g	Total (mg)	mg/g
60	330	25	11.27	0.63	0.01	3.59	0.06

#### 4. Conclusions and Recommendations

The potential of MBC prepared in-house at two temperatures, 900 °C and 1000 °C, was tested for nitrate removal as a model for nutrient removal in agricultural runoff. Kinetic experiments and structural analyses were applied to select a suitable biochar for further testing in a column system design. MBC prepared at 1000 °C was found to have a rougher texture and to be more crystalline compared to the one prepared at 900 °C, however the 1000 °C MBC had slightly lower functional groups as opposed to the 900 °C MBC. These characteristics allowed the MBC prepared at 1000 °C to have a higher nitrate removal rate.

It was found that nitrate removal was significantly affected by both concentration and flowrate and their interactions with each other. A maximum removal capacity of 0.11 mg/g NO<sub>3</sub><sup>-</sup> (which corresponds to a removal percentage of more than 45%, representing the adsorption capacity at equilibrium) was obtained at the highest concentration and lowest flowrate. Examination of the characteristics of the MBC before and after adsorption and adsorption kinetics, indicated that the hydroxyl functional group on the MBC surface interacted with NO<sub>3</sub><sup>-</sup> and contributed to its removal. MBC with higher crystallinity, texture roughness and conductivity had higher NO<sub>3</sub><sup>-</sup> removal, indicating the importance of these characteristics in nitrate adsorption with biochar. It was found that the column arrived at the breakthrough point at the 25 min mark and was exhausted by 330 min, where the unused length of bed reached 11.27 cm out of a total of 12.2 cm (≈92% saturated) for a total adsorption of 3 mg of NO<sub>3</sub><sup>-</sup>. The prepared macadamia biochar in this study showed promising results for nitrate removal. However, to have a comprehensive evaluation of the use of this recycled waste for agricultural runoff treatment, ways of improving the performance of the char, in terms of regeneration and nutrients recovery, are recommended as areas for exploration in future work. It is also recommended that MBC potency for agricultural runoff treatment and nutrients recovery be tested on a large scale with natural water samples to prove its feasibility for such an application.

**Author Contributions:** R.A.A.-J. conducted design of experiments, provided instructions and recommendations for analytical techniques for characterization, helped with data analyses and interpretation and refined the last draft. S.B. conducted experiments, data collection and analyses and put together the first draft. L.B. contributed to biochar production and design of experimental setup as well as English editing.

**Funding:** This research received no external funding.

**Acknowledgments:** The first author is grateful for the financial support he received from the Ministry of Water Resources in Iraq and the University of Southern Queensland. The authors would like also to acknowledge Stafford McKnight from Federation University Australia for his support in XRD measurements and analysis. The authors are also thankful to Susan SA Alkurdi for her help in FTIR measurements.

**Conflicts of Interest:** The authors declare no conflicts of interest.

#### References

1. Kleinman, P.J.A.; Sharpley, A.N.; Moyer, B.G.; Elwinger, G.F. Effect of Mineral and Manure Phosphorus Sources on Runoff Phosphorus. *J. Environ. Qual.* **2002**, *31*, 2026–2033. [[CrossRef](#)] [[PubMed](#)]
2. Beman, J.M.; Arrigo, K.R.; Matson, P.A. Agricultural runoff fuels large phytoplankton blooms in vulnerable areas of the ocean. *Nature* **2005**, *434*, 211–214. [[CrossRef](#)] [[PubMed](#)]
3. Hafshejani, L.D.; Hooshmand, A.; Naseri, A.A.; Mohammadi, A.S.; Abbasi, F.; Bhatnagar, A. Removal of nitrate from aqueous solution by modified sugarcane bagasse biochar. *Ecol. Eng.* **2016**, *95*, 101–111. [[CrossRef](#)]
4. Chintala, R.; Mollinedo, J.; Schumacher, T.E.; Papiernik, S.K.; Malo, D.D.; Clay, D.E.; Kumar, S.; Gulbrandson, D.W. Nitrate sorption and desorption in biochars from fast pyrolysis. *Microporous Mesoporous Mater.* **2013**, *179*, 250–257. [[CrossRef](#)]
5. Xu, X.; Gao, B.Y.; Yue, Q.Y.; Zhong, Q.Q. Preparation of agricultural by-product based anion exchanger and its utilization for nitrate and phosphate removal. *Bioresour. Technol.* **2010**, *101*, 8558–8564. [[CrossRef](#)] [[PubMed](#)]

6. Zhang, M.; Gao, B.; Yao, Y.; Xue, Y.; Inyang, M. Synthesis of porous MgO-biochar nanocomposites for removal of phosphate and nitrate from aqueous solutions. *Chem. Eng. J.* **2012**, *210*, 26–32. [CrossRef]
7. Water\_Online. About Nutrient Removal. 2017. Available online: <https://www.wateronline.com/solution/nutrient-removal> (accessed on 15 July 2019).
8. Good, A.G.; Beatty, P.H. Fertilizing Nature: A Tragedy of Excess in the Commons. *PLoS Biol.* **2011**, *9*, e1001124. [CrossRef] [PubMed]
9. Bhatnagar, A.; Kumar, E.; Sillanpää, M. Nitrate removal from water by nano-alumina: Characterization and sorption studies. *Chem. Eng. J.* **2010**, *163*, 317–323. [CrossRef]
10. Olgun, A.; Atar, N.; Wang, S. Batch and column studies of phosphate and nitrate adsorption on waste solids containing boron impurity. *Chem. Eng. J.* **2013**, *222*, 108–119. [CrossRef]
11. Plant Health Australia. Macadamias. 2012. Available online: <http://www.planthealthaustralia.com.au/about-us/> (accessed on 29 June 2019).
12. Fan, F.; Yang, Z.; Li, H.; Shi, Z.; Kan, H. Preparation and properties of hydrochars from macadamia nut shell via hydrothermal carbonization. *R. Soc. Open Sci.* **2018**, *5*, 181126. [CrossRef]
13. Bada, S.; Falcon, R.; Falcon, L.; Makhula, M. Thermogravimetric investigation of macadamia nut shell, coal, and anthracite in different combustion atmospheres. *J. South. Afr. Inst. Min. Met.* **2015**, *115*, 741–746. [CrossRef]
14. Kumar, U.; Maroufi, S.; Rajarao, R.; Mayyas, M.; Mansuri, I.; Joshi, R.K.; Sahajwalla, V. Cleaner production of iron by using waste macadamia biomass as a carbon resource. *J. Clean. Prod.* **2017**, *158*, 218–224. [CrossRef]
15. Wrobel-Tobiszewska, A.; Boersma, M.; Sargison, J.; Adams, P.; Singh, B.; Franks, S.; Birch, C.J.; Close, D.C. Nutrient changes in potting mix and Eucalyptus nitens leaf tissue under macadamia biochar amendments. *J. For. Res.* **2018**, *29*, 383–393. [CrossRef]
16. Spokas, K.A.; Baker, J.M.; Reicosky, D.C. Ethylene: Potential key for biochar amendment impacts. *Plant Soil* **2010**, *333*, 443–452. [CrossRef]
17. Roser, M.B.; Feyereisen, G.W.; Spokas, K.A.; Mulla, D.J.; Strock, J.S.; Gutknecht, J. Carbon Dosing Increases Nitrate Removal Rates in Denitrifying Bioreactors at Low-Temperature High-Flow Conditions. *J. Environ. Qual.* **2018**, *47*, 856–864. [CrossRef] [PubMed]
18. Roser, M. Using Unique Carbon Source Combinations to Increase Nitrate and Phosphate Removal in Bioreactors. Master's Thesis, University of Minnesota, Minneapolis, MN, USA, 2016.
19. Yang, J.; Li, H.; Zhang, D.; Wu, M.; Pan, B. Limited role of biochars in nitrogen fixation through nitrate adsorption. *Sci. Total Environ.* **2017**, *592*, 758–765. [CrossRef] [PubMed]
20. Beutel, M.W.; Newton, C.D.; Brouillard, E.S.; Watts, R.J. Nitrate removal in surface-flow constructed wetlands treating dilute agricultural runoff in the lower Yakima Basin, Washington. *Ecol. Eng.* **2009**, *35*, 1538–1546. [CrossRef]
21. Lang, M.; Li, P.; Yan, X. Runoff concentration and load of nitrogen and phosphorus from a residential area in an intensive agricultural watershed. *Sci. Total Environ.* **2013**, *458*, 238–245. [CrossRef]
22. Ghane, E.; Ranaivoson, A.Z.; Feyereisen, G.W.; Rosen, C.J.; Moncrief, J.F. Comparison of Contaminant Transport in Agricultural Drainage Water and Urban Stormwater Runoff. *PLoS ONE* **2016**, *11*, e0167834. [CrossRef]
23. Department of Primary Industries. Farm Water Quality and Treatment. 2014. Available online: [https://www.dpi.nsw.gov.au/\\_\\_data/assets/pdf\\_file/0013/164101/Farm-water-quality-and-treatment.pdf](https://www.dpi.nsw.gov.au/__data/assets/pdf_file/0013/164101/Farm-water-quality-and-treatment.pdf) (accessed on 1 June 2019).
24. Bae, J.S.; Su, S. Macadamia nut shell-derived carbon composites for post combustion CO<sub>2</sub> capture. *Int. J. Greenh. Gas Control* **2013**, *19*, 174–182. [CrossRef]
25. Nick, T. Benefits of Biochar and its Applications for Runoff Water Management: Literature Review and Laboratory Report. Bachelor Thesis, Novia University of Applied Sciences, Vaasa, Finland, 2018.
26. Shackley, S.; Sohi, S.; Brownsort, P.; Carter, S.; Cook, J.; Cunningham, C.; Gaunt, J.; Hammond, J.; Ibarrola, R.; Mašek, O. An Assessment of the Benefits and Issues Associated with the Application of Biochar to Soil. In *A Report Commissioned by United Kingdom Department for Environment, Food and Rural Affairs, and Department of Energy and Climate Change*; 2010; p. 132.
27. Hagemann, N.; Spokas, K.; Schmidt, H.-P.; Kägi, R.; Böhler, M.A.; Bucheli, T.D. Activated Carbon, Biochar and Charcoal: Linkages and Synergies across Pyrogenic Carbon's ABCs. *Water* **2018**, *10*, 182. [CrossRef]

28. Shen, Y.S.; Wang, S.L.; Huang, S.T.; Tzou, Y.M.; Huang, J.H. Biosorption of Cr(VI) by coconut coir: Spectroscopic investigation on the reaction mechanism of Cr(VI) with lignocellulosic material. *J. Hazard. Mater.* **2010**, *179*, 160–165. [[CrossRef](#)] [[PubMed](#)]
29. Coates, J. Interpretation of infrared spectra, a practical approach. *Encycl. Anal. Chem.* **2000**, *12*, 10815–10837.
30. Eaton, A.; Clesceri, E.W.; Rice, A.E.; Greenberg, M.J.C.E.; Franson; APHA; AWWA; WEF. *Standard Methods for the Examination of Water and Wastewater*; APHA: Washington, DC, USA, 2005.
31. Inyang, M.; Gao, B.; Wu, L.; Yao, Y.; Zhang, M.; Liu, L. Filtration of engineered nanoparticles in carbon-based fixed bed columns. *Chem. Eng. J.* **2013**, *220*, 221–227. [[CrossRef](#)]
32. Zhao, H.; Xue, Y.; Long, L.; Hu, X. Adsorption of nitrate onto biochar derived from agricultural residuals. *Water Sci. Technol.* **2018**, *77*, 548–554. [[CrossRef](#)] [[PubMed](#)]
33. Ho, Y.; McKay, G. Pseudo-second order model for sorption processes. *Process. Biochem.* **1999**, *34*, 451–465. [[CrossRef](#)]
34. Martins, A.C.; Pezoti, O.; Cazetta, A.L.; Bedin, K.C.; Yamazaki, D.A.; Bandoch, G.F.; Asefa, T.; Visentainer, J.V.; Almeida, V.C. Removal of tetracycline by NaOH-activated carbon produced from macadamia nut shells: Kinetic and equilibrium studies. *Chem. Eng. J.* **2015**, *260*, 291–299. [[CrossRef](#)]
35. Mandal, S.; Thangarajan, R.; Bolan, N.S.; Sarkar, B.; Khan, N.; Ok, Y.S.; Naidu, R. Biochar-induced concomitant decrease in ammonia volatilization and increase in nitrogen use efficiency by wheat. *Chemosphere* **2016**, *142*, 120–127. [[CrossRef](#)] [[PubMed](#)]
36. Joseph, S.; Kammann, C.I.; Shepherd, J.G.; Conte, P.; Schmidt, H.-P.; Hagemann, N.; Rich, A.M.; Marjo, C.E.; Allen, J.; Munroe, P.; et al. Microstructural and associated chemical changes during the composting of a high temperature biochar: Mechanisms for nitrate, phosphate and other nutrient retention and release. *Sci. Total Environ.* **2018**, *618*, 1210–1223. [[CrossRef](#)]
37. Sanford, J.; Larson, R.; Runge, T. Nitrate sorption to biochar following chemical oxidation. *Sci. Total Environ.* **2019**, *669*, 938–947. [[CrossRef](#)]
38. Fidel, R.B.; Laird, D.A.; Spokas, K.A. Sorption of ammonium and nitrate to biochars is electrostatic and pH-dependent. *Sci. Rep.* **2018**, *8*, 17627. [[CrossRef](#)] [[PubMed](#)]
39. Patnaik, P.; Khoury, J.N. Reaction of phenol with nitrite ion: Pathways of formation of nitrophenols in environmental waters. *Water Res.* **2004**, *38*, 206–210. [[CrossRef](#)] [[PubMed](#)]
40. Cimo, G.; Haller, A.; Spokas, K.; Novak, J.; Ippolito, J.; Löhnertz, O.; Kammann, C. Mechanisms of Nitrate Capture in Biochar: Are they Related to Biochar Properties, Post-Treatment and Soil Environment? In Proceedings of the 19th EGU General Assembly Conference Abstracts, Vienna, Austria, 23–28 April 2017.
41. Gai, X.; Wang, H.; Liu, J.; Zhai, L.; Liu, S.; Ren, T.; Liu, H. Effects of Feedstock and Pyrolysis Temperature on Biochar Adsorption of Ammonium and Nitrate. *PLoS ONE* **2014**, *9*, e113888. [[CrossRef](#)] [[PubMed](#)]
42. Rafiq, M.K.; Bachmann, R.T.; Shang, Z.; Joseph, S.; Long, R. Influence of Pyrolysis Temperature on Physico-Chemical Properties of Corn Stover (*Zea mays* L.) Biochar and Feasibility for Carbon Capture and Energy Balance. *PLoS ONE* **2016**, *11*, e0156894. [[CrossRef](#)] [[PubMed](#)]
43. Kang, D.S.; Lee, S.M.; Lee, S.H.; Roh, J.S. X-ray diffraction analysis of the crystallinity of phenolic resin-derived carbon as a function of the heating rate during the carbonization process. *Carbon Lett.* **2018**, *27*, 108–111.
44. Rajarao, R.; Mansuri, I.; Dhunna, R.; Khanna, R.; Sahajwalla, V. Study of structural evolution of chars during rapid pyrolysis of waste CDs at different temperatures. *Fuel* **2014**, *134*, 17–25. [[CrossRef](#)]
45. Al-Juboori, R.A.; Yusaf, T.; Aravinthan, V.; Bowtell, L. Investigating natural organic carbon removal and structural alteration induced by pulsed ultrasound. *Sci. Total Environ.* **2016**, *541*, 1019–1030. [[CrossRef](#)] [[PubMed](#)]
46. Ryan, B.F.; Joiner, B.L.; Cryer, J.D. *MINITAB Handbook: Update for Release*; Cengage Learning: Boston, MA, USA, 2012.
47. Boubakri, A.; Helali, N.; Tlili, M.; Ben Amor, M. Fluoride removal from diluted solutions by Donnan dialysis using full factorial design. *Korean J. Chem. Eng.* **2014**, *31*, 461–466. [[CrossRef](#)]
48. Mondal, M. Removal of Pb(II) ions from aqueous solution using activated tea waste: Adsorption on a fixed-bed column. *J. Environ. Manag.* **2009**, *90*, 3266–3271. [[CrossRef](#)]

49. Xing, X.; Gao, B.Y.; Zhong, Q.Q.; Yue, Q.Y.; Li, Q. Sorption of nitrate onto amine-crosslinked wheat straw: Characteristics, column sorption and desorption properties. *J. Hazard. Mater.* **2011**, *186*, 206–211. [[CrossRef](#)]
50. Karunaratne, H.; Amarasinghe, B. Fixed Bed Adsorption Column Studies for the Removal of Aqueous Phenol from Activated Carbon Prepared from Sugarcane Bagasse. *Energy Procedia* **2013**, *34*, 83–90. [[CrossRef](#)]



© 2019 by the authors. Licensee MDPI, Basel, Switzerland. This article is an open access article distributed under the terms and conditions of the Creative Commons Attribution (CC BY) license (<http://creativecommons.org/licenses/by/4.0/>).